المجلة العلمية لجامعة الملك فيصل
The Scientific Journal of King Faisal University
العلوم الأساسية والتطبيقية
Basic and Applied Sciences

Surface Water Body Extraction Using Landsat 8 Images and Different Forms of Physical Models

Tanutdech Rotjanakusol and Teerawong Laosuwan

Department of Physics, Faculty of Science, Mahasarakham University, Kham Riang, Kantarawichai, Maha Sarakham, 44150, Thailand

KEYWORDS الكلمات المفتاحية
Sonca, satellite data, ndvi, ndwi, mndwi, wri

ACCEPTED القبول
10/05/2020

PUBLISHED النشر
01/12/2020

https://doi.org/10.37575/b/sci/2100

ABSTRACT

Floods are natural disasters or phenomena that often occur in different areas of Thailand. During August 2017, Kalasin province, which is located in the central north-eastern area of Thailand, was affected by tropical storm Sonca, resulting in heavy rainfall and floods. These floods had a tremendous impact on the way of life of the people in the area, as well as resulting in damage to agricultural areas. The objectives of this research are to propose a method of surface water body extraction from Landsat 8 data, together with four different forms of physical models: 1) the Normalised Difference Vegetation Index, 2) the Normalised Difference Water Index, 3) the Modified Normalised Difference Water Index, and 4) the Water Ratio Index (WRI). The result of the research found that the data analysis from satellite Landsat 8, together with the WRI physical model, was the most reliable method. The overall classification accuracy was equivalent to 94.44%, and the kappa statistic was equivalent to 0.8154. In addition, this method could also efficiently specify the water area from the land area.

1. Introduction

A natural disaster or natural phenomenon results in a tremendous impact on humankind from damage to property to loss of lives. Additionally, it also results in the deterioration of society (Milly, 2005; Krausmann et al., 2008; Brunda and Nyamathi, 2015). Some of the most frequently occurring natural disasters are floods, being equivalent to 41.4%, followed by earthquakes and storms, respectively. The Asian region often suffers the most extreme effects (DDPM, 2013). In Thailand, the cost of damage from floods increased from 6,000 million baht (18,885,744 USD) in 1990 to 40 billion baht (1,317,663,600 USD) in 2004 and 1.44 trillion baht (47,435,889,600 USD) in 2011 (ADRC, 2012). The flood that occurred in Thailand in 2011 has been ranked fourth as the incident that caused the most damage in the world after the earthquake and tsunami in Japan in 2011, the earthquake in Japan in 1995, and Hurricane Katrina in the United States in 2005, respectively (TMD, 2017). Thailand covers an area of 513,115 km^2 and is situated in the heart of Indochina, in Southeast Asia. In the past, Thailand has encountered flood problems every year in all regions of the country. The reason for this is geographical as Thailand is located in the tropics. Thus, the country has been affected by both the southwest and the northeast monsoons. There are also storms that pass over country yearlong (Amini, 2010). There is an urgent necessity for evaluation of the severity of the floods and the damage they cause in terms of information or maps displaying the disaster area (Blanc et al., 2012; Kia et al., 2012; Saini and Kaushik, 2012; Kim et al., 2014; Elkhrachy, 2015). Furthermore, the traditional method that includes ground surveying is expensive and takes a long time. It is also difficult to access large areas.

The applied use of remote sensing technology from satellite data can record different phenomena on the planet using the reflection of electromagnetic waves to sensors installed on the satellite (Laosuwan and Uttaruk, 2016; Krishnan et al., 2017; Uttaruk and Laosuwan, 2017; Al-husban, 2018; Rotjanakusol and Laosuwan, 2018). It can also be used, together with the physical model, as a tool to evaluate the severity of a flood. Satellite data is able to cover and access large surface areas and the costs can be minimal when compared with ground surveying (Rokni et al., 2014; Ledien et al., 2017; Sarp and Ozcelik, 2017; Acharya et al., 2018).

At the beginning of August 2017, the Rong Kham district, in Kalasin province, which is situated in the north-eastern part of Thailand, encountered heavy rainfall due to the influence of tropical storm Sonca. The heavy rainfall resulted in the major flooding that affected the lives of the people in the area, and damaged the agricultural area considerably (Thaiwater, 2017; TMD, 2017).For the aforementioned reasons, this research aims to propose the surface water body extraction method from satellite Landsat 8, together with the use of four different types of physical models including 1) the Normalised Difference Vegetation Index (NDVI), 2) the Normalised Difference Water Index (NDWI), 3) the Modified Normalised Difference Water Index (MNDWI), and 4) the Water Ratio Index (WRI). The flooding incident in the Rong Kham district, Kalasin province, in 2017 will be used as a case study.

2. Operation Area and Data

2.1. Study Area:

Kalasin Province (Fig. 1) is one of the four provinces of the central north-eastern region of Thailand and is located at approximately 16°–17°N latitude and 103°–104°E longitude, having a total area of 6,946.746 km^2.

Fig. 1. The Study Area

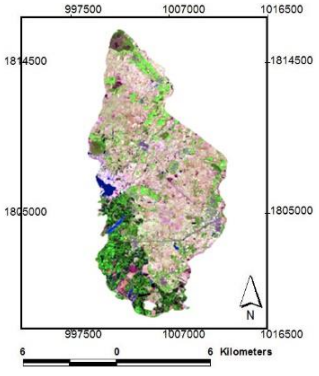

Corresponding Author: Teerawong Laosuwan teerawong@msu.ac.th ,0066854181011

The average temperature throughout the year is approximately 26.40°C, and the average amount of rainfall throughout the year is 1,259.80 mm. The study area for this research is the Rong Kham district, Kalasin province, with a total area of 82.137 km^2.

2.2. Data from a Satellite:

Landsat 8 satellite is a satellite for the exploration of natural resources from the United States Geological Survey (USGS). It was developed as a result of collaboration between NASA and the USGS. It went into orbit on 11 February 2013. The satellite is capable of recording repeated data at the same location every 16 days. It also consists of two types of data records, which are Operational Land Imager (OLI) and Thermal Infrared Sensor (TIR) totalling 11 wavelengths, as shown in Table 1. For this research, Landsat 8 satellite (path 128 row 49) was used to cover the case study area of the Rong Kham district, Kalasin province. The satellite recorded data as follows: 1) before the flood (19 February 2017), 2) during the flood (30 August 2017), and 3) after the flood (29 December 2017). For this study, the data were downloaded from EarthExplorer at: https://earthexplorer.usgs.gov/

Table 1. Specifications of the Landsat 8 OLI/TIR Satellite/Sensor Wavelength (μm) Name Resolution

Satellite/Sensor	Wavelength (μm)	Name	Resolution
Landsat 8 OLI/TIR	Band 1: 0.43 - 0.45	Coastal aerosol	30 m
	Band 2: 0.45 - 0.51	Blue	30 m
	Band 3: 0.53 - 0.59	Green	30 m
	Band 4: 0.64 - 0.67	Red	30 m
	Band 5: 0.85 - 0.88	NIR	30 m
	Band 6: 1.57 - 1.65	SWIR-1	30 m
	Band 7: 2.11 - 2.35	SWIR-2	30 m
	Band 8: 0.50 - 0.68	Panchromatic	15 m
	Band 9: 1.36 - 0.38	Cirrus	30 m
	Band 10: 10.60 -11.19	Thermal IR 1	100 m
	Band 11: 11.50 - 12.51	Thermal IR2	100 m

Source: (USGS, 2013)

2.3. Rainfall Data:

In this research, the study gathered monthly rainfall data (for the same period as the satellite data) that was measured by a rainfall gauging station on the ground by the Thai Meteorological Department (TMD) for the total of 12 stations covered in the Kalasin province area. The monthly rainfall data will be used to compare with the analysed result from the satellite data with four types of the physical models.

3. Materials and Methods

The process in this research is shown in Fig. 2. The objective was to display the area that changed during the flood. The research will analyse the data in the three periods that are 1) before the flood, 2) during the flood, and 3) after the flood; it will use four forms of physical models to analyse the data from the three periods and this can be explained as follows.

Fig. 2. Process of this research

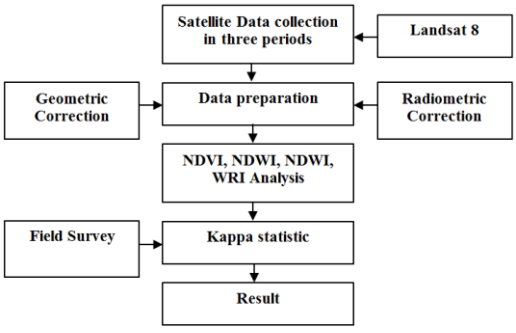

3.1. Normalised Difference Vegetation Index (NDVI) Analysis:

The NDVI analysis was proposed by Rouse et al. (1973). The NDVI is the calculation of the ratio between the difference and the sum of the reflection of the red wave and between the near infrared (NIR) waves of the material on the surface. The result of the calculation will provide a value of the NDVI between -1 to +1. The plant-covered area will have a high reflection of NIR wave over the red wave. This results in the NDVI becoming positive. By contrast, surfaces that are soil, bare land, and construction areas will have a higher reflected value between the two similar waves. This will result in the NDVI value being close to zero. In the case in which the surface is water, the reflection for the infrared wave will be lower than the visible wavelength. This will result in the red wave being visible and the NDVI being negative. The NDVI calculation is shown according to Equation 1.

$$NDVI=\frac{NIR-RED}{NIR-RED} \quad (1)$$

Where

NIR = Near infrared wavelength (Band 5)

RED = Red wavelength (Band 4)

3.2 Normalised Difference Water Index (NDWI) Analysis:

The NDWI analysis was proposed by McFeeters (1996). The NDWI is the calculation for the ratio between the difference and sum of the green wave and the NIR wave of the material on the earth's surface. The result will be used to categorise the water on the soil's surface. The result of the NDWI will be a value between -1 to +1; this will help with the analysis and categorisation of water-covered areas and make it easier than previously. This can especially apply areas with an NDWI value of between -1 to 0, i.e. referring to areas with vegetation. These vegetation-covered areas will have an NDWI that is close to a value of +1 value, i.e., similar to water-covered areas. The calculation of NDWI is shown in Equation 2.

$$NDWI=\frac{GREEN-NIR}{GREEN+NIR} \quad (2)$$

Where

GREEN = Green wavelength (Band 3)

NIR = Near infrared wavelength (Band 5)

3.3 Modified Normalised Difference Water Index (MNDWI) Analysis:

The MNDWI analysis was proposed by Xu (2006). The MNDWI was developed to accurately differentiate between the soil-covered and water-covered areas. It uses the spectral enhancement of the material in the water-covered area on the land's surface and helps to reduce the waves from construction sites, vegetation, and soil. The MNDWI is the calculation of the ratio between the difference and the sum that reflects the green wavelength and the MIR wavelength. The result of the MNDWI calculation will have a value between -1 to +1. Water will have a more positive value than a NDWI resulting from absorption when the MIR wavelength is more than the NIR. The soil's surface and plant-covered areas will have negative values as the soil will be reflected by the MIR wavelength compared with the NIR. The vegetation will also be reflected in the MIR wavelength more than in the green wavelength. The MNDWI calculation, is shown in Equation 3.

$$MNDWI=\frac{GREEN-MIR}{GREEN+MIR} \quad (3)$$

Where

GREEN = Green wavelength (Band 3)

MIR = Middle infrared wavelength or SWIR1 wavelength (Band 6)

3.4 Water Ratio Index (WRI) Analysis:

The WRI analysis was proposed by Shen and Li, (2010). The WRI is the calculation of the ratio between the difference and the sum of the reflection of the red wavelength and the green wavelength. When comparing this with the NIR wavelength and the MIR wavelength, the WRI value will have a lowest value of 0 and will increase in value. The WRI value will be close to 0. Highly plant-covered areas, where the WRI value is close to, and more than, 1, are referred to as water areas. The WRI calculation, is shown in Equation 4.

$$WRI=\frac{GREEN+RED}{NIR+MIR} \quad (4)$$

Where

GREEN = Green wavelength (Band 3)

RED = Red wavelength (Band 4)

NIR = Near infrared wavelength (Band 5)

MIR = Middle Infrared wavelength or SWIR1 wavelength (Band 6)

For the data analysis in the initial process, we used the analysis results from the four types of physical models mentioned for the ground surveying. The survey area specified covered 60 areas. The areas were spread across the case study. In the last stage, the accuracy will be evaluated using the kappa statistic. If the kappa statistic is more than 80%, this shows that the data analysis result is highly accurate. If the kappa statistic is between 40%–80%, this shows that the data analysis result is moderately accurate. If the kappa statistic is less than 40%, this shows that the data analysis result is accurate at a low level.

4. Results and Discussion

4.1. Satellite Data Analysis Result:

The satellite data analysis results of Landsat 8 satellite with four types of physical models – 1) NDVI 2) NDWI 3) MNDWI, and 4) WRI – can be shown and discussed as follows:

NDVI Analysis Result: The NDVI is the calculation of the ratio between the difference and the sum of reflection value for the red wavelength and the NIR wavelength. The NDVI has a value between -1 to +1. The data analysis for this research will be from: 1) before the flood, 2) during the flood, and 3) after the flood as shown in Table 2.

Table 2. NDVI analysis

Periods	Min	Max	Mean	StdDev
Before Flood	-0.541	0.757	0.369	0.122
During Flood	-0.532	0.769	-0.337	0.289
After Flood	-0.686	0.759	0.372	0.101

For the convenience of spatial analysis, the research will categorise the NDVI analysis results into five periods as follows: 1) data having a value of between -1.000 to -0.600, and the value refers to an area with a large surface of water, 2) data having a value of between -0.60 to -0.200, and the value refers an area with a small amount of water, 3) data having a value of between -0.20 to 0.200, and the value refers to areas with small quantities of vegetation, 4) data having a value between 0.200 to 0.600, and the value refers to areas with moderate vegetation, and 5) data having a value of between 0.600 to 1.000, and the value refers to areas covered with a large amount of vegetation. The NDVI physical model was analysed with spatial analysis method and it was found that:

- Before the flood. The first period was equivalent to an area of 0.671 km^2. The second period had the area that was equivalent to 0.305 km^2, and the third period had an area that was equivalent to 1.0818 km^2. The fourth period had an area that was equivalent to 67.663, km^2, and the fifth period had an area that was equivalent to 12.416 km^2.
- During the flood. The first period had an area that was equivalent to 13.351 km^2. The second period had an area that was equivalent to 1.760 km^2. The third period had an area that was equivalent to 1.196 km^2. The fourth period had an area that is equivalent to 4.993 km^2, and the fifth period had an area that was equivalent to 60.837 km^2.
- After the flood. The first period had an area that was equivalent to 1.129 km^2. The second period had an area that was equivalent to 0.616 km^2. The third period had an area that was equivalent to 1.337 km^2. The fourth period had an area that was equivalent to 54.896 km^2, and the fifth period had an area that was equivalent to 24.159 km^2. The results of the categorisation of the NDVI were calculated in the form of spatial analysis based on the case study and are shown in Fig. 3.

Fig. 3. Spatial analysis of the NDVI in the Rong Kham district, Kalasin province

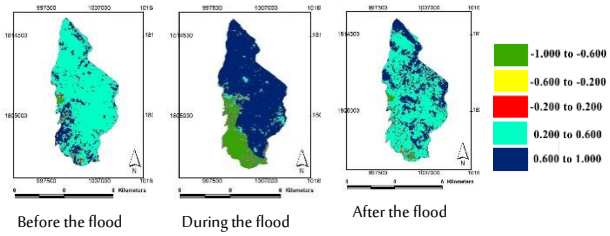

Additionally, after the analysis of the NDVI was taken to compare with the rainfall, it was found that 1) Before the flood; the amount of the measured rainfall was equivalent to 0.0 mm (without rainfall). The average of the NDVI was equivalent to 0.122; this can be explained as when there was no rainfall, the average of the NDVI would decrease due to there being a smaller plant-covered area. 2) During the flood; the amount of measured rainfall was equivalent to 132.7 mm; the NDVI had an average that was equivalent to -0.337. This can be explained as when the amount of rainfall increases, the average of the NDVI will be negative as more water covers the area. 3) After the flood; the amount of measured rainfall was equivalent to 2.1 mm; the NDVI average was equivalent to 0.372; this can be explained as a decreased amount of rainfall would result in a decrease of the NDVI average, which will have a lower value due to the small plant-covered area.

NDWI Analysis Result: NDWI is the calculation of the ratio between the difference and the sum for the reflection of the green wavelength and the NIR wavelength. The NDWI, according to the definition, will be between -1 to +1 similar to the NDVI, but it will display the opposite result. The area with an NDWI value close to +1 will be shown as an area of water. If NDWI value is closer to -1 than to 0, this will refer to a plant-covered area. The data analysis results for this research were before the flood, during the flood, and after flood, as shown in Table 3.

Table 3. NDWI analysis

Periods	Min	Max	Mean	StdDev
Before Flood	-0.511	0.692	-0.445	0.046
During Flood	-0.461	0.898	0.343	0.547
After Flood	-0.523	0.889	-0.436	0.056

The spatial analysis in this research categorised the NDWI physical model into five periods as follows: 1) the first period with a value between -1.000 to -0.600; this will refer to a highly plant-covered area, 2) the second period will have a value between -0.600 to -0.200; this will refer to a moderately plant-covered area, 3) the third period will have a value between -0.200 to 0.200; this will refer to low plant-covered area, 4) the fourth period will have a value between 0.200 to 0.600; this will refer to an area with a low to moderate amount of water, and 5) the fifth period will have a value between 0.600 to

1.000; this will refer to an area with a high amount of water. After taking the NDWI physical model in the spatial analysis, the result found that:

- Before the flood. The first data had an area that was equivalent to 35.233 km^2. The second data had an area that was equivalent to 25.883 km^2. The third data had an area that was equivalent to 19.738 km^2. The fourth data had an area that was equivalent to 1.053 km^2, and the fifth data had an area that was equivalent to 0.230 km^2.
- During the flood. The first data had an area that was equivalent to 1.709 km^2. The second data had an area that was equivalent to 4.551 km^2. The third data had an area that was equivalent to 59.638 km^2. The fourth data had an area that was equivalent to 5.453 km^2, the fifth data had an area that was equivalent to 10.786 km^2.
- After the flood. The first data had an area that was equivalent to 13.712 km^2. The second data had an area that was equivalent to 20.929 km^2. The third data had an area that was equivalent to 45.921 km^2. The fourth data had an area that was equivalent to 0.002 km^2, and the fifth data had an area that was equivalent to 1.581 km^2. Thus, the result of the categorisation of the NDWI was calculated according to spatial analysis of the case study area as shown in Fig. 4.

Fig. 4. Spatial analysis of the NDWI in the Rong Kham district, Kalasin province

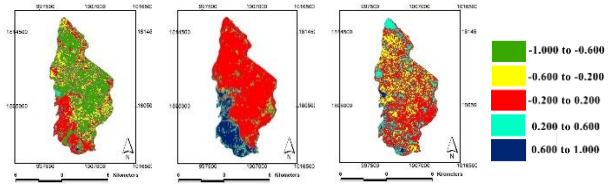

In addition, the NDWI analysis results when used to compare with the amount of rainfall found that:

- Before the flood. The amount of rainfall was equivalent to 0.0 mm (no rainfall). The NDWI average was equivalent to -0.047; this can be explained as when there was no rainfall, the NDWI average would be less due to a lesser area being water-covered.
- During the flood. The amount of measured rainfall was equivalent to 132.7 mm; the average of the NDWI was equivalent to 0.472; this can be explained as when the amount of the rainfall increases, the average NDWI will increase as will be an increased amount of rainfall.
- After the flood. The amount of measured rainfall was equivalent to 2.1 mm; the average of the NDWI was equivalent to -0.011; this can be explained as when the rainfall decreased, the average value of the NDWI would decrease due to there being a smaller water-covered area.

MNDWI Analysis Result: As mentioned earlier, the MNDWI is a method that helps to differentiate water in the soil or plants from the amount of sunray that reflects from the soil or plants during the green wavelength and the MIR wavelength. The calculation of MNDWI will give three results:

- Water will have a more positive value than the NDWI as the absorption during the MIR wavelength would be more than the NIR wavelength,
- The soil area will have a negative value,
- The soil and plants will retain a negative value due to the fact that soil reflects during the MIR wavelength more than during the NIR wavelength, and plants reflect more during the MIR wavelength than during the green wavelength. The MNDVI consists of a value between -1 to +1, similar to the NDWI. For the research, the data analysis results are shown for before the flood, during the flood, and after the flood, as shown in Table 4.

Table 4. MNDWI analysis

Periods	Min	Max	Mean	StdDev
Before Flood	-0.511	0.692	-0.445	0.046
During Flood	-0.461	0.898	0.343	0.547
After Flood	-0.523	0.889	-0.436	0.056

For the spatial analysis in this research, the MNDWI physical model can be categorised into five periods as follows: 1) the first period with a value between -1.000 to -0.600; this refers to a highly plant-covered area, 2) the second period with a value between -0.600 to -0.200; this refers to a moderately plant-covered area, 3) the third with a value between -0.200 to 0.200; this refers to an area with a low level of plant cover, 4) the fourth period will have a value of between 0.200 to 0.600; this refers to an area with a low to moderate amount of water, and 5) the fifth period will have a value between 0.600 to 1.000; this refers to an area with a high amount of water. After taking the MNDWI physical model in the spatial analysis, the results found that:

- Before the flood. The first data had an area that was equivalent to 77.491 km^2. The second data had an area that was equivalent to 2.697 km^2. The third data had an area that was equivalent to 0.723 km^2. The fourth data had an area that was equivalent to 0.371 km^2, and the fifth data had an area that was equivalent to 0.855 km^2.
- During the flood. The first data had an area that was equivalent to 64.067 km2. The second data had an area that was equivalent to 1.025 km2. The third data had an area that was equivalent to 1.291 km2. The fourth data had an area that was equivalent to 1.528 km2, and the fifth data had an area that was equivalent to 14.266 km2.
- After the flood. The first data had an area that was equivalent to 62.046 km^2. The second data had an area that was equivalent to 13.621 km^2. The third data had an area that was equivalent to 2.967 km^2. The fourth data had an area that was equivalent to 2.052 km^2 and the fifth data had an area that was equivalent to 1.451 km^2. Thus, the results of the categorisation of the MNDWI as calculated in the spatial analysis of the case study area are as shown in Fig. 5.

Fig. 5. Spatial analysis of the MNDWI in the Rong Kham district, Kalasin province

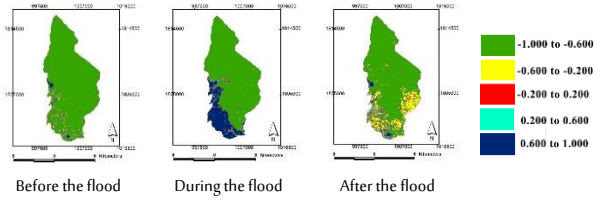

In addition, the MNDWI analysis result when used to compare with the amount of rainfall found that:

- Before the flood. The amount of rainfall was equivalent to 0.0 mm (no rainfall). The MNDWI average was equivalent to -0.445; this can be explained as when there was no rainfall, the MNDWI average would be less due to there being a smaller water-covered area.
- During the flood. The amount of measured rainfall was equivalent to 132.7 mm; the average of the MNDWI was equivalent to 0.343; this can be explained as when the amount of the rainfall increases, the average MNDWI would increase as there was an increasing amount of rainfall.
- After the flood. The amount of measured rainfall was equivalent to 2.1 mm; the average of the MNDWI was equivalent to -0.436; this can be explained as when the rainfall decreased, the average value of the MNDWI would decrease due to there being a smaller water-covered area.

WRI Analysis Result: The WRI physical model was developed to differentiate water by calculating the difference and the sum for the reflection of the red wavelength and the green wavelength compared with the NIR wavelength and the MIR wavelength. The WRI, according to the definition, will have a value that differs from the NDVI, NDWI, and MNDWI. Thus, if the MRI is close to 0, this will refer to an area that is highly plant-covered. If the WRI value is close to, and more than, 1, this will refer to an area with water. The data analysis results for the research can be shown for before the flood, during the flood, and after the flood, as shown in Table 5.

Table 5. WRI analysis

Periods	Min	Max	Mean	StdDev
Before Flood	0.250	5.478	0.468	0.215
During Flood	0.208	5.637	1.021	1.431
After Flood	0.236	8.047	0.529	0.293

The spatial analysis in this research categorised the WRI physical model into five periods as follows: 1) the first period with a value between -1.000 to -0.600; this refers to a highly plant-covered area, 2) the second period will have a value between -0.600 to -0.200; this refers to a moderately plant-covered area, 3) the third period will have a value between -0.200 to 0.200; this refers to an area with a low amount of plant cover, 4) the fourth period will have a value between 0.200 to 0.600; this refers to an area with low to moderate amount of water, and 5) the fifth period will have a value between 0.600 to 1.000; this refers to an area with a high amount of water. After taking the WRI physical model in the spatial analysis, the results found that:

- Before the flood. The first data had an area that was equivalent to 81.014 km^2. The second data had an area that was equivalent to 0.497 km^2. The third data had an area that was equivalent to 0.175 km^2. The fourth data had an area that was equivalent to 0.098 km^2, and the fifth data had an area that was equivalent to 0.353 km^2.
- During the flood. The first data had an area that was equivalent to 65.918 km^2. The second data had an area that was equivalent to 2.374 km^2. The third data had an area that was equivalent to 2.948 km^2. The fourth data had an area that was equivalent to 6.039 km^2, and the fifth data had an area that was equivalent to 4.858 km^2.
- After the flood. The first data had an area that was equivalent to 80.477 km^2. The second data had an area that was equivalent to 0.564 km^2. The third data had an area that was equivalent to 0.428 km^2. The fourth data had an area that was equivalent to 0.368 km^2, and the fifth data had an area that was equivalent to 0.330 km^2. Thus, the results of the categorisation of the WRI were calculated in spatial analysis of the case study area, as shown in Fig. 6.

Fig. 6. Spatial analysis of the WRI in the Rong Kham district, Kalasin province

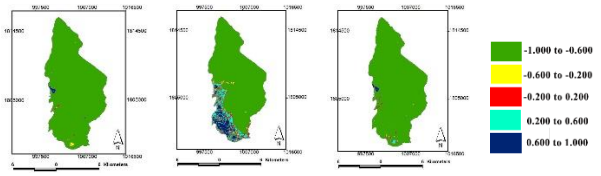

In addition, the WRI analysis result when used to compare with the amount of rainfall found that: 1) Before the flood, the amount of rainfall was equivalent to 0.0 mm (no rainfall). The WRI average was equivalent to 0.468; this can be explained as when there was no rainfall, the WRI average would be less due to there being a smaller water-covered area, 2) During the flood, the amount of measured rainfall was equivalent to 132.7 mm; the average of the WRI was equivalent to 1.021; this can be explained as when the amount of the rainfall increases, the average WRI would increase as there was an increasing amount of rainfall, 3) After the flood, the amount of measured rainfall was equivalent to 2.1 mm; the average of the WRI was equivalent to 0.529; this can be explained as when the rainfall decreased, the average value of the WRI would decrease due to there being a smaller water-covered area.

4.2. Result of Ground Surveying and Accuracy Evaluation Metric:

The accuracy evaluation metric in this research will take into consideration the result of the categorisation; especially the water area and the soil area. The four types of physical models are NDVI, NDWI, MNDWI, and WRI based on 60 observation areas (ground survey area). This was explained as follows: 1) The NDVI physical model found that the overall classification accuracy was equivalent to 92.22%, and the kappa statistic was equivalent to 0.8736, 2) The NDWI physical model found that the overall classification accuracy was equivalent to 90.00%, and the kappa statistics was equivalent to 0.8204, 3) The MNDWI physical model found that the overall classification accuracy was equivalent to 82.22%, and the kappa statistic was equivalent to 0.7240, and 4) The WRI physical model found that the overall classification accuracy was equivalent to 94.44%, and the kappa statistic was equivalent to 0.8154.

After considering the overall classification accuracy from the four different physical models, the WRI was found to have the highest accuracy in the data analysis. Fig.7 shows the spatial data before the flood, during the flood, and after the flood with the WRI physical model.

Fig. 7. Spatial analysis of the WRI

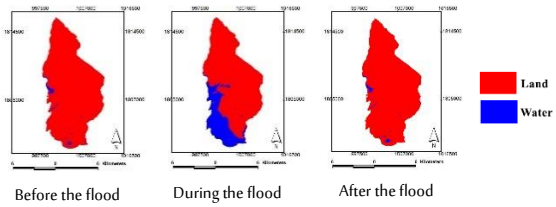

From Fig. 7, it can be explained that the comparison of the spatial data analysis of the WRI before the flood has a water area that was equivalent to 0.549% or equivalent to 0.451 km^2. The soil area was also equivalent to 99.451% or equivalent to 81.686 km^2. During the flood, the water area was equivalent to 7.897 km^2 and the soil area was equivalent to 86.733% or equivalent to 74.240 km^2. After the flood, the water area was equivalent to 0.850% or equivalent to the area of 0.850 km^2. The soil area was equivalent to 99.150%, which was equivalent to 81.287 km^2. The comparison of data for the WRI clearly shows the differences before the flood, during the flood and after the flood.

5. Conclusions

Thailand is under the influence of two types of monsoons i.e. the southwest monsoon and the northeast monsoon; this is why Thailand has two seasons that are the wet and the dry seasons. The dry season can be divided into two sub-seasons, summer and winter. The seasons in Thailand can be categorised into three seasons: summer, rainy, and winter seasons. Tropical storm Sonca was the ninth tropical cyclone for the Pacific typhoon season in 2017. This typhoon resulted in heavy rainfall and caused a vast amount of damage to the north-eastern part of Thailand during 26–29 July 2017. The research focused on the proposal of a surface water body extraction method that is suitable for this region, especially in the central north-eastern part of Thailand. During the flood incident in 2017, The Rong Kham district, Kalasin province, during the flood incident 2017, is a case study in which the data has been applied from the Landsat 8 satellite, together with the use of four types of physical models, which are the NDVI, the NDWI, the MNDWI, and the WRI. The results of the study were used to compare with similar research such as the research by Rokni et al., (2014); Ledien et al., (2017); Sarp and Ozcelik (2017); Acharya et al., (2018), that found that the research results from these four topics have similar conclusions as this research. The result of the research was a good criterion and was able to rationally evaluate areas that were covered with water. This could be further used for the inspection of, and immediate warning for, flooding areas. Related sectors could use this method to analyse flood areas and use the results to further create a sustainable flood prevention and rescue plan.

Acknowledgements

The author would like to thank United States Geological Survey (Earth Explorer) for satellite data, Miss. Jiratchaya Khosombat and Miss. Paweena Bekunthod for data collection.

Bios

Tanutdech Rotjanakusol

Department of Physics, Faculty of Science, Mahasarakham University, Kham Riang, Kantarawichai, Maha Sarakham, 44150, Thailand, 0066835565464, tanutdech.r@msu.ac.th

Tanutdech Rotjanakusol took M.Sc. Physics in 2013 from Suranaree University of Technology, Thailand. He is a Lecturer and Research in the Department of Physics, Faculty of Science, Mahasarakham University. Author and co-author of more than 20 scientific papers in the areas of Physics, Remote Sensing, Geoinformatics, etc.

Teerawong Laosuwan

Department of Physics, Faculty of Science, Mahasarakham University, Kham Riang, Kantarawichai, Maha Sarakham, 44150, Thailand, 0066854181011, teerawong@msu.ac.th

Teerawong Laosuwan, Ph.D. in Electrical and Computer Engineering from Mahasarakham University, associate professor of the Department of Physics, Faculty of Science, Mahasarakham University, Thailand. He has worked on various projects, such as drought and flood risk management, climate change mitigation and adaptation, etc. Author and co-author of more than 70 scientific papers in the areas of Remote Sensing, Geoinformatics, Digital Image Processing, etc.

References

Acharya, T.D., Subedi, A. and Lee, D.H. (2018). Evaluation of water indices for surface water extraction in a Landsat 8 scene of Nepal. *Sensors*, **18**(8), 2580.

Al-husban, Y. (2018). Meandering and land use/cover change detection in the lower Jordan river, 1984-2016, using GIS and RS. *Environmental Research, Engineering and Management*, **74**(2), 34–51.

Amini, J. (2010). A method for generating floodplain maps using IKONOS images and DEMs. *International Journal of Remote Sensing*, **31**(9), 2441–56.

Asian Disaster Reduction Center (ADRC). (2012). *Natural Disaster Data Book*. Available at: http://www.adrc.asia/publications/databook/DB2012_e.html (Accessed on 02/01/2013)

Blanc, J., Hall, J., Roche, N., Dawson, R., Cesses, Y., Burton, A. and Kilsby, C. (2012). Enhanced efficiency of pluvial flood risk estimation in urban areas using spatial-temporal rainfall simulations. *Journal of Flood Risk Management*, **5**(2),143–52.

Brunda, G.S. and Nyamathi, S.J. (2015). Derivation and analysis of dimensionless hydrograph and s curve for cumulative watershed area. *Aquatic Procedia*, **4**(n/a), 964–71.

Department of Disaster Prevention and Mitigation (DDPM). (2013). *Annual Report 2013*. Available at: http://www.disaster.go.th/th/dwn-download-12-1/ (Accessed on 07/11/2013)

Elkhrachy, I. (2015). Flash flood hazard mapping using satellite images and gis tools: a case study of Najran city, Kingdom of Saudi Arabia (KSA). *The Egyptian Journal of Remote Sensing and Space Science*, **18**(2), 261–78.

Kia, M.B., Pirasteh, S., Pradhan, B., Mahmud, A.R., Sulaiman, W.N.A., and Moradi, A. (2012). An artificial neural network model for flood simulation using GIS: Johor River Basin, Malaysia. *Environmental Earth Sciences*, **67**(1), 1–14.

Kim, B., Sanders, B.F., Schubert, J.E. and Famiglietti, J.S. (2014). Mesh type tradeoffs in 2D hydrodynamic modeling of flooding with a Godunov-based flow solver. *Advances in Water Resources*, **68**(n/a), 42–61.

Krausmann, E. and Mushtaq, F. (2008). A qualitative Natech dam¬age scale for the impact of floods on selected industrial facilities. *Natural Hazards*, **46**(2), 179–97.

Krishnan, N.M.V., Mohan, S.M.A., Pratheesh, P., Vijith. H. (2017). Performance evaluation and sensitivity analysis of ASTER and SRTM (30m) DEM derived terrain variables in landslide susceptibility assessment: A case from the Western Ghats. *Environmental Research, Engineering and Management*, **73**(2), 21–40.

Laosuwan, T., Uttaruk, Y. (2016). Application of geo-informatics and vegetation indices to estimate above-ground carbon sequestration. *Studia Universitatis Vasile Goldis Arad, Seria*, 26(4), 449–54

Ledien, J., Sorn, S., Hem, S., Huy, R., Buchy, P., Tarantola, A. and Cappelle, J. (2017). Assessing the performance of remotely-sensed flooding indicators and their potential contribution to early warning for leptospirosis in Cambodia. *PLOS ONE*, **12**(7), 1–15.

McFeeters, S.K. (1996). The use of normalized difference water index (NDWI) in the delineation of open water features. *International Journal of Remote Sensing*, **17**(n/a), 1425–32.

Milly, P.C., Wetherald, R.T., Dunne, K.A. and Delworth, T.L. (2002). Increasing risk of great floods in a changing climate. *Nature*, **415**(6871), 514–7.

Rokni, K., Ahmad, A., Selamat, A., Hazini, S. (2014). Water feature extraction and change detection using multitemporal Landsat imagery. *Remote Sensing*, **6**(5), 4173–89.

Rotjanakusol, T., Laosuwan, T. (2018). Remote sensing based drought monitoring in the middle-part of northeast region of Thailand. *Studia Universitatis Vasile Goldis Arad, Seria Stiintele Vietii*, **28**(1), 14–21.

Rouse, J.W., Haas, R.H., Schell, J.A. and Deering, D.W. (1973). Monitoring vegetation systems in the Great Plains with ERTS (earth resources technology satellite). In: *Third Earth Resources Technology Satellite Symposium*. Greenbelt, ON, Canada, 10–14/12/1973, pp. 309–17.

Saini, S.S., and Kaushik, S.P. (2012). Risk and vulnerability assessment of flood hazard in part of Ghaggar Basin: A case study of Guhla block, Kaithal, Haryana, India. *International Journal of Geomatics and Geosciences*, **3**(1), 42–54.

Sarp, G., and Ozcelik, M. (2017). Water body extraction and change detection using time series: A case study of Lake Burdur, Turkey. *Journal of Taibah University for Science*, **11**(3), 381–91.

Shen, L., and Li, C. (2010). Water body extraction from Landsat ETM imagery using adaboost algorithm. In: *18th International Conference on Geoinformatics*, Beijing, China, 18-20/06/2010, pp. 1–4.

Thai Meteorological Department (TMD). (2017). *Meteorological Book 2017*. Available at: https://www.tmd.go.th/info/info.php?FileID=70 (Accessed on 09/10/2017)

Thai Meteorological Department (TMD). (2017). *SONCA*. Available at: http://www.thaiwater.net/current/ 2017/SONCAjuly 2017/sonca.html (Accessed on 11/10/2017)

Thaiwater. (2017). *SONCA*. Available at: https://www.tmd.go.th/warningwindow.php?wID=6099 (Accessed on 11/10/2017)

USGS. (2013). *Landsat 8 Band Designations*. Available at: https://www.usgs.gov/media/images/landsat-8-band-designations (Accessed on 01/05/2017)

Uttaruk, Y. and Laosuwan, T. (2017). Drought detection by application of remote sensing technology and vegetation phenology. *Journal of Ecological Engineering*, **18**(6), 115–21.

Xu, H. (2006). Modification of normalized difference water index (NDWI) to enhance open water features in remotely sensed imagery. *International Journal of Remote Sensing*, **27**(14), 3025–33.